Running title: Complete life cycle of the bioluminescent California Sea Firefly

Laboratory culture of the California Sea Firefly *Vargula tsujii* (Ostracoda: Cypridinidae): Developing a model system for the evolution of marine bioluminescence

Jessica A. Goodheart[1], Geetanjali Minsky[1], Mira N. Brynjegard-Bialik[1], Michael S. Drummond[1], J. David Munoz[2], Timothy R. Fallon[3,4], Darrin T. Schultz[5,6], Jing-Ke Weng[3,4], Elizabeth Torres[2] & Todd H. Oakley*[1]

[1] Department of Ecology, Evolution, and Marine Biology, University of California, Santa Barbara, Santa Barbara, CA 93106

[2] Department of Biological Sciences, California State University, Los Angeles, CA 90032-8201, USA

[3] Whitehead Institute for Biomedical Research, Cambridge, MA, 02142, USA

[4] Department of Biology, Massachusetts Institute of Technology, Cambridge, MA 02142, USA

[5] Monterey Bay Aquarium Research Institute, Moss Landing, CA 95060, USA

[6] Department of Biomolecular Engineering and Bioinformatics, University of California, Santa Cruz, Santa Cruz, CA 96060, USA

*Corresponding author: oakley@ucsb.edu

Abstract

Bioluminescence, or the production of light by living organisms via chemical reaction, is widespread across Metazoa. Culture of bioluminescent organisms from diverse taxonomic groups is important for determining the biosynthetic pathways of bioluminescent substrates, which may lead to new tools for biotechnology and biomedicine. Some bioluminescent groups may be cultured, including some cnidarians, ctenophores, and brittle stars, but those use luminescent substrates (luciferins) obtained from their diets, and therefore are not informative for determination of the biosynthethic pathways of the luciferins. Other groups, including terrestrial fireflies, do synthesize their own luciferin, but culturing them is difficult, and the biosynthetic pathway for firefly luciferin remains unclear. An additional independent origin of endogenous bioluminescence is found within ostracods from the family Cypridinidae, which use their luminescence for defense and, in Caribbean species, for courtship displays. Here, we report the first complete life cycle of a luminous ostracod (*Vargula tsujii* Kornicker & Baker, 1977, the California Sea Firefly) in the laboratory. We also describe the late-stage embryogenesis of *Vargula tsujii* and discuss the size classes of instar development. We find embryogenesis in *V. tsujii* ranges from 25-38 days, and this species appears to have five instar stages, consistent with ontogeny in other cypridinid lineages. We estimate a complete life cycle at 3-4 months. We also present the first complete mitochondrial genome for *Vargula tsujii*. Bringing a luminous ostracod into laboratory culture sets the stage for many potential avenues of study, including learning the biosynthetic pathway of cypridinid luciferin and genomic manipulation of an autogenic bioluminescent system.

Keywords: ostracod, cypridinid, animal culture, cypridinid luciferin, embryogenesis, Crustacea

53 **Introduction**

54 The production of bioluminescence in animals is an important biological phenomenon that is
55 particularly prevalent in marine environments [1]. To produce light, animals combine an enzyme
56 (usually a luciferase or photoprotein) and a substrate (luciferin) with oxygen, and sometimes
57 additional components such as ATP or calcium [2–4]. Although the enzymes that produce light are
58 well-studied [5–13], and we know how the substrate is produced in bacteria [14] and fungi [15], we do
59 not yet know how luciferin is synthesized in any animal system. A comprehensive understanding
60 of this pathway could be transformative for optogenetics in transgenic organisms, where the
61 ability to produce bioluminescence in situ as a biosensor or light source would be invaluable.
62 Some laboratory-reared luminescent animals already exist (Table 1), but may not be suitable for
63 studying luciferin biosynthesis. In particular, ctenophores, cnidarians, and brittle stars use
64 coelenterazine obtained from their diet as a substrate [1]. Fireflies do use an endogenous luciferin
65 specific to Coleoptera (beetles) [16], but they often have longer life cycles than other taxa, slowing
66 research progress [17]. Although there are other independent origins of autogenic
67 bioluminescence, which we define as that produced via luciferase and luciferin that are
68 synthesized via the genome of the light producing animal, no laboratory cultures of these
69 animals currently exist. This makes additional studies focused on the comparative evolution of
70 this ability extremely challenging.

71

72 Ostracods from the family Cypridinidae independently evolved bioluminescence, and use a
73 luciferin that is endogenous to ostracods and chemically different from that of other
74 bioluminescent organisms [2,18,19]. Of the metazoan taxa already cultured, autogenic
75 luminescence is only known to occur within fireflies [20,21]. Due to the independent origin of
76 ostracod bioluminescence in the family Cypridinidae, and evidence for the autogenic nature of
77 the necessary luciferin and luciferase, ostracods represent an importantl lineage for
78 understanding how bioluminescence evolved. Establishing laboratory cultures of luminescent

79 ostracods within Cypridinidae will provide opportunities for new investigations into the
80 biosynthetic pathway of luciferins in Metazoa, as well as comparative studies of the
81 biochemistry, physiology, genetics, and function of endogenous bioluminescence.
82
83 **Table 1.** Species of bioluminescent metazoans for which cultures are known to exist, including
84 information on the luciferin used for luminescence, estimated generation times, and whether the
85 luciferin used is synthesized via the genome of the luminescent organism itself (autogenic).

Species	**Phylum**	**Luciferin**	**Autogenic luciferin?**	**Generation time**	**Citations**
Mnemiopsis leidyi, Bolinopsis infundibulum, Leucothea pulchra	Ctenophora	coelenterazine	Possibly	~13 days (based on *M. mccradyi*)	[85–88]
Clytia haemispherica	Cnidaria	coelenterazine	No	~14 days (based on other *Clytia*)	[70,89]
Amphiura filiformis	Echinodermata	coelenterazine	No	Unknown	[90]
Photuris spp. Aspisoma lineatum Aquatica lateralis Aquatica ficta	Arthropoda	beetle luciferin	Yes	3-24 months	[17,74,75,91]
Arachnocampa richardsae	Arthropoda	glow worm luciferin	Possibly	10-12 months	[92–94]
Pontodrilus litoralis	Annelida	earthworm luciferin	?	1-3 months	[95]
Oikopleura dioica	Chordata	?	?	5 days	[96,97]

86

87 Cypridinidae is estimated to include over 300 ostracod species [22], some of which use
88 bioluminescence for defense, while others possess the ability to create bioluminescent courtship
89 displays in addition to defensive secretions [23]. Lineages with sexually dimorphic bioluminescent
90 displays, such as those in Cypridinidae, have more species than their non-displaying sister
91 lineages, indicating that origins of bioluminescent courtship may increase diversification rates [24].
92 As such, cypridinid ostracods represent an excellent system for understanding how behavioral
93 diversification can lead to increases in species accumulation. Furthermore, cypridinid ostracods
94 diversified while generating bioluminescence with a consistent biochemical basis across the
95 clade [25], meaning that they use the same luciferin and homologous enzymes to make light. The
96 conserved nature of the luminescent chemical reaction provides a system within which
97 bioluminescence can produce rapid changes in phenotypic diversity by modifying amino acid
98 sequences of the enzyme and how the enzyme is used [26].

99

100 Attempts to culture luminescent and non-luminescent species of Cypridinidae have led to
101 varying success, including *Skogsbergia lerneri* (non-luminous species with no mating in culture)
102 [27], *Photeros annecohenae* (luminous species without the complete life cycle in culture) [28], and
103 *Vargula hilgendorfii* (luminous species with no mating in culture) [29]. Researchers attempting to
104 culture *Vargula hilgendorfii* tried multiple alternative aquarium set-ups and tested sensitivity to
105 nutrients commonly measured in aquaria, but were still unable to induce mating in the lab [29]. An
106 unnamed species of luminescent ostracod is claimed to have been cultured at the CTAQUA
107 Foundation (Aquaculture and Technological Centre) in Spain for molecular gastronomy [30], but
108 no information on species, culture longevity, or whether mating occurred is available on this
109 enigmatic and uncertain culture. Other non-cypridinid ostracods have been reared in the
110 laboratory as well, including the myodocopids *Euphilomedes carcharodonta* [31] and
111 *Euphilomedes nipponica* [32] and the podocopids *Xestoleberis hanaii* and *Neonesidea*

oligodentata [33] (only records of copulation in the laboratory for any ostracods) [34]. Many podocopids grow quite easily in aquaria, so a number of other species have been cultured for descriptions of, or experiments related to, post-embryonic development, including *Chlamydotheca incisa* and *Strandesia bicuspis* [35], *Heterocypris salina* [36–38], *Eucypris virens* [37], and *Candona rawsoni* [38].

In this paper, we present evidence that we are the first to rear a luminous ostracod (*Vargula tsujii* Kornicker & Baker, 1977) through its complete life cycle in the laboratory. *Vargula tsujii* is the only bioluminescent cypridinid ostracod described from the Pacific coast of North America. Commonly found in southern California, the reported range of *V. tsujii* is from Baja California to Monterey Bay [39]. This species is demersal (moves between the benthic and planktonic environments) and is primarily active in or near the kelp forest at night [40]. Similarly to some other cypridinid ostracods, *Vargula tsujii* is a scavenger, and is presumed to feed on dead and decaying fish and invertebrates on the benthos since they can be collected via baited traps. In addition, some authors observed *V. tsujii* attacking the soft tissues of live fishes caged nearshore [41]. *Vargula tsujii* is an important prey item of the plainfin midshipman fish (*Porichthys notatus*), as it is the source of luciferin for the bioluminescence seen in the fish [42].

In addition to evidence for the completion of the life cycle of *Vargula tsujii* in the laboratory, we provide a successful methodology for culturing populations of *V. tsujii*, descriptions and analyses of late stage embryogenesis and instar development, a reconstruction of its mitochondrial genome, and a brief description of the distribution of molecular diversity of *V. tsujii* across coastal southern California.

Methods

Specimen collection

We collected *Vargula tsujii* from three primary locations at 0-10 m depth: (1) Fisherman's Cove near Two Harbors on Catalina Island, CA, USA (33°26'42.5"N 118°29'04.2"W) directly adjacent to the Wrigley Marine Science Center, (2) Cabrillo Marina, Los Angeles, CA, USA (33°43'13.5"N 118°16'47.4"W), and (3) Shelter Island public boat ramp, San Diego, CA, USA (32°42'56.3"N 117°13'22.9"W) (Figure 1; Table S1). We also provide locations in Figure 1 and Table S1 where we set traps but did not collect *V. tsujii*. The specimens used for culture and description of the life cycle of *V. tsujii* were exclusively from Fisherman's Cove, Catalina Island, and we collected additional specimens from the Cabrillo Marina and Shelter Island public boat ramp to discern the genetic diversity of *V. tsujii* and test for the presence of any cryptic species. For specimen collection we used Morin pipe traps: cylindrical polyvinyl chloride (PVC) tubes with mesh funnels to prevent the ostracods from escaping once they entered [43]. We baited traps with dead fish or fresh chicken liver (roughly 1-2 cm^3). We set traps in 1-10 meters of water at sunset and collected them 1.5 to 2 hours after last light to allow time for the ostracods to accumulate.

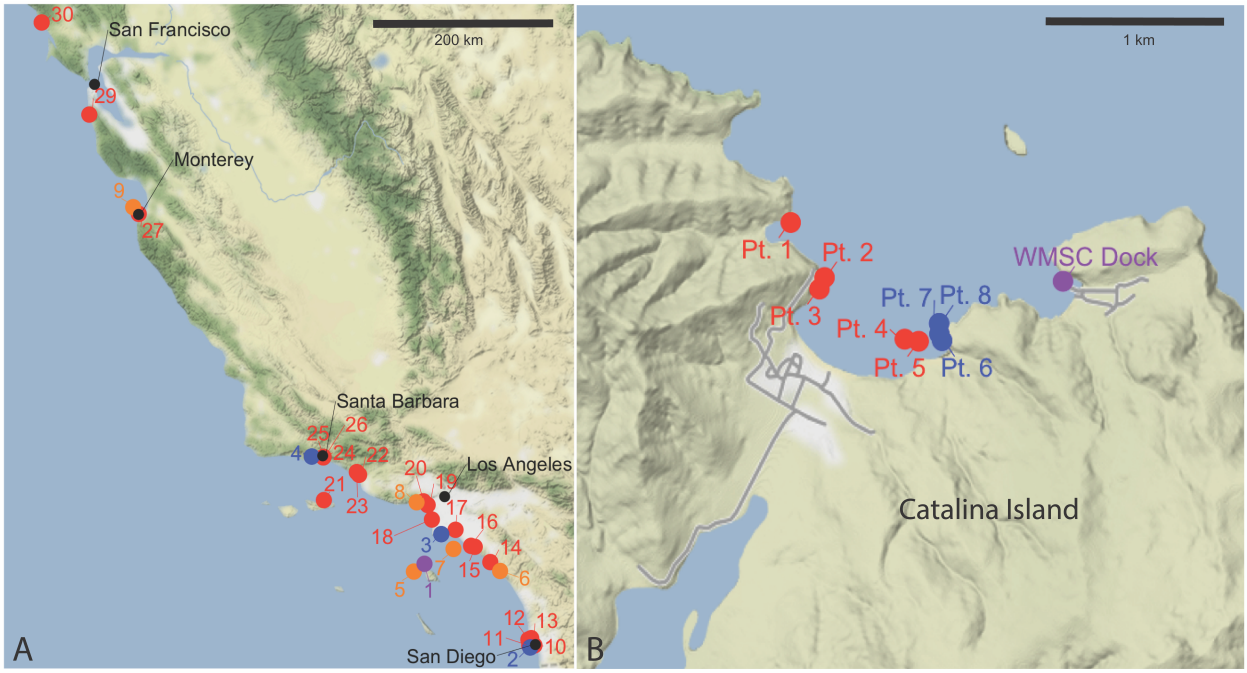

Figure 1. Map of localities where collections (and attempted collections of Vargula tsujii were made). Black points represent geographic annotations for reference, purple points refer to the location where ostracods were collected that were ultimately cultured, blue where animals were found or collected, orange where Kornicker originally collected animals, and red where no V. tsujii were found. (A) Map of the California (USA) coastline where V. tsujii collections were attempted; (B) Map of the region near Two Harbors (Santa Catalina Island, California, USA) where V. tsujii collections were attempted.

Population genetic analyses

We obtained *Vargula tsujii* sequence data for 16S rRNA (16S) and cytochrome oxidase 1 (COI) from a previously published thesis [44]. We then aligned and visually inspected sequence chromatograms with Sequencher version 3.1 (Gene Codes Corp) (Table S1). We constructed haplotype networks for the two genes, COI (Number of individuals: Catalina, 18; San Diego, 11; San Pedro, 12) and 16S (Number of individuals: Catalina, 19; San Diego, 20; San Pedro, 21) with the package pegas [45] in the R environment (version 3.4.2) [46]. To assess whether sequences within populations cluster together, we analyzed each gene via Discriminant Analysis of Principal Components (DAPC) using the adegenet package in R [47] and compared models with one, two, and three clusters using the Bayesian Information Criterion (BIC) [48].

Description of aquarium system and feeding

We cultured *Vargula tsujii* at the University of California, Santa Barbara in aquariums designed for water to flow through sand and out the bottom. This allowed continuous water flow to keep water fresh, and not suck ostracods into a filter. Instead, ostracods remain in sand where they spend the daylight hours. We kept animals under a 12:12 light cycle with an indirect blue LED light.

We first modified a five gallon glass tank by drilling a hole in the bottom, which was then covered with the bottom of an undergravel filter and a 3 cm layer of commercial aragonite sand with grain sizes 1-2 mm for aquariums (CaribSea brand). To maintain continuous water flow, we used plastic tubing (diameter = 1 cm) connected directly to an overflowing reservoir tank, itself fed by UCSB's seawater system that pumps directly from the Pacific. The tube from the reservoir created a siphon system for moving water into the main tank (Figure 2). The siphon

180 provided continuous water flow when needed, and prevented overflow of the aquarium. In
181 addition, to prevent a complete drain of the water if the siphon flow broke, which is common with
182 larger siphons, we attached an outflow pipe to the bottom of the aquarium that drained halfway
183 up the side of the tank (Figure 2).
184
185 We also created a similar system for smaller experimental aquaria, but these appeared to be
186 less effective long-term, as we saw high mortality in non-systematic studies. For the small
187 aquaria ("condos"), we cut a large hole (~5 cm diameter) into the bottom of 500 mL Nalgene™
188 Square PETG Media Bottles with Septum Closures (Figs. 2F, S7). We then modified a 100 μm
189 cell strainer to fit in the bore of the media bottle in such a way that it would remain there when
190 the closure of the media bottle was screwed back on, allowing water but not sand to flow
191 through. We inverted the bottle and added a ~3 cm layer of sand above the cell strainer,
192 measured from the edge of the bottle cap. In plain terms, the condos are simply capped bottles,
193 turned upside down, after creating a large hole in the bottom and a small hole in the cap. There
194 is a strainer in the cap so water can flow down through the cap and not get clogged by sand.
195 For these smaller aquaria, we used 5 mm diameter tubing as siphons from the reservoir tank
196 and for the outflow. Similar to the large tank, the outflow tubes (placed in the septum closure)
197 drained roughly halfway up the side of the aquaria to prevent the water from draining
198 completely.
199
200 Most recently, we created custom aquariums from acrylic (Fig. 2G), with similar dimensions to
201 the 5-gallon glass aquarium. We installed a bulkhead in the bottom and attached PVC tubing as
202 a drain, which we again raised to about half the height of the aquarium to prevent complete
203 drainage if inflow of water stops accidentally. We added a valve to control the rate of outflow
204 and instead of a siphon, we added a float switch to set inflow rate. Currently, we raise the

outflow pipe to set the level of water in the aquarium and use continuous inflow directly to the main aquarium, which works well as long as the water is draining freely. We use a flow rate of approximately 0.4 L/min.

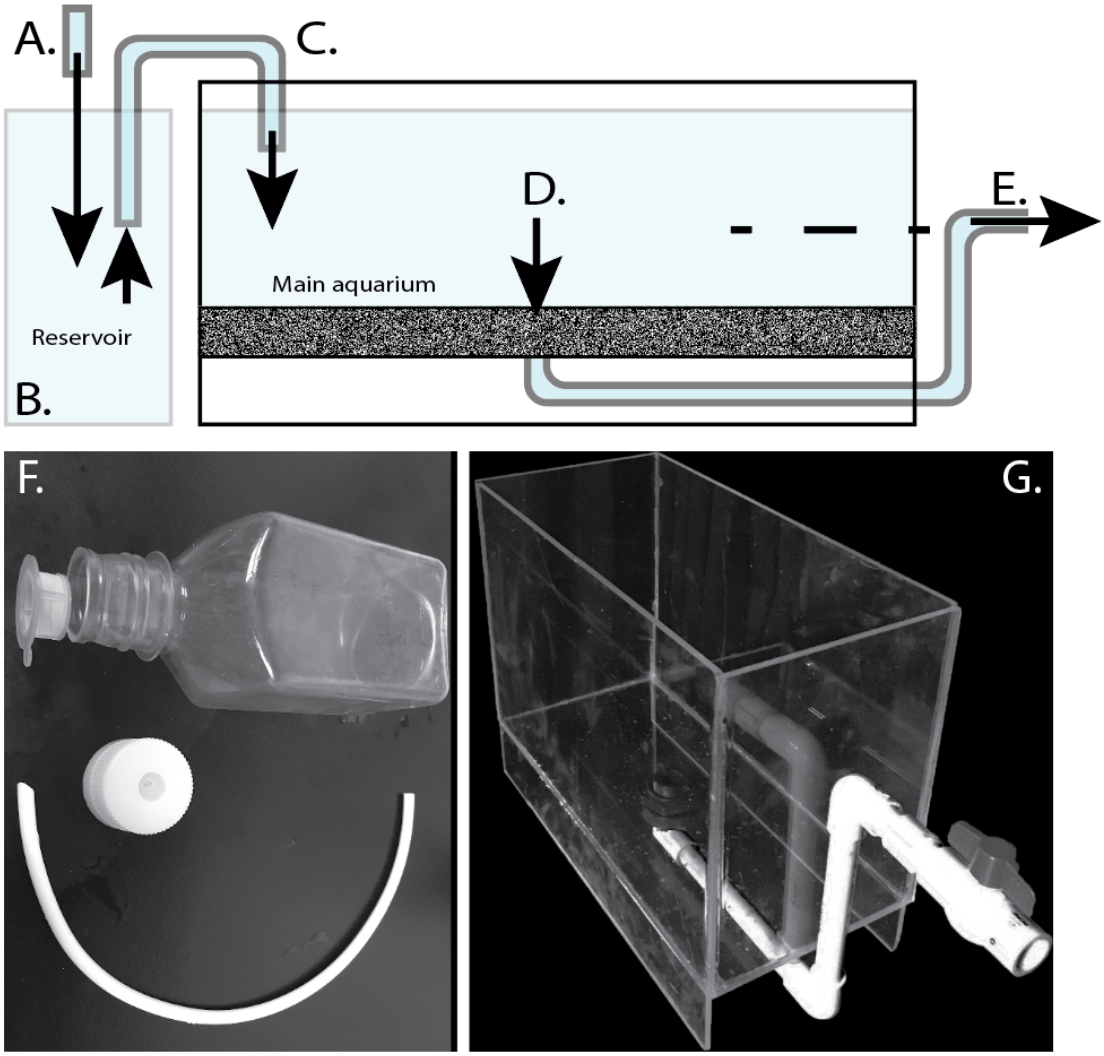

Figure 2. Diagrammatic representation of aquarium setup for sea fireflies. (A) Source water flows into (B) a reservoir tank, which overflows to keep the reservoir full and water level constant. (C) We use a siphon to carry water from a reservoir tank to main aquarium where ostracods live. Water level of the main tank drains through sand (stippled), through (E) an outflow that is raised to a level that would cause water to remain at the level of the dashed line, even if a siphon is interrupted to cause water to stop flowing into the main tank. (F) Plastic bottle and parts used to create small aquarium using the same logic as main aquarium. (G) Custom-built acrylic aquarium with drain in bottom and raised outflow with adjustable rate.

215 We initially offered the ostracods multiple diet choices, including: (1) imitation crab, which is
216 primarily pollock, (2) carnivore fish pellets or fish flakes, (3) tilapia fillets, and (4) anchovies,
217 which have each made for successful food sources in Caribbean ostracods (Todd Oakley,
218 personal observation; [28,43]). Although the adults appeared moderately interested in these food
219 sources in non-systematic trials, we found the juvenile ostracods did not eat them, but they did
220 actively feed on raw chicken liver, as do *Vargula hilgendorfii* individuals from Japan [49]. In
221 culture, we therefore provided pieces of chicken liver daily (~1 cm^3 per 200 animals). Due to the
222 nocturnal life history of *V. tsujii*, we fed them in the late afternoon or early evening (around the
223 beginning of the dark cycle), and removed the food from the aquarium in the morning (~3-5
224 hours into the light cycle) to reduce the chance of bacterial fouling.
225
226 *Rearing of embryos*
227 We tested two primary methods for rearing embryos. The first was less successful in terms of
228 longevity of both the mothers and embryos, but provided usable data on embryogenesis.
229 Regardless of rearing method, ostracods did not appear to eat while they were brooding.
230
231 For the first method, we kept females individually in circular wells in twelve-well dishes [28], with
232 approximately 1 mL of 17°C seawater. We recorded visual observations of the females and their
233 embryos and changed the water daily. The advantage of this method is ease of identification
234 and observation of individual ostracods, allowing us to track the growth of specific embryos over
235 a given period of time. However, all females which deposited embryos into the brooding
236 chamber died before their embryos were released from the marsupium, although the precise
237 cause of death is unknown. These embryos were then removed from the female marsupium by
238 dissection, kept in wells, and observed until the animals hatched through the chorion (see
239 Supplemental Video).

240

241 For the second method, we identified and removed brooding females from the aquarium and
242 placed them in 50 mL Falcon™ tubes (2 females per tube). Roughly 5 mL of commercial
243 aragonite sand for saltwater aquariums with most grain sizes 1.0-2.0 mm (Caribsea brand) was
244 added to the bottom of each tube to allow females to burrow. Falcon tubes were then placed in
245 a large seawater reservoir that ranged from 17-19°C. We changed the water in each tube daily,
246 and imaged brooding females every other day with a camera attached to a dissecting scope.
247 We used key diagnostic features such as number of embryos and female size to distinguish
248 individual females from one another. Of the thirteen individuals kept in Falcon™ tubes, only one
249 died prior to embryo release from the marsupium.

250

251 *Animal measurements and inferences of instar size classes*

252 We imaged ostracods across all life stages using a standard dissecting microscope and an
253 Olympus brand camera, and measured the carapace length, carapace height, eye width, and
254 keel width with the software Fiji (Sample size = 626 individuals; Table S3) [50]. These parameters
255 are useful in the determination of the instar stages in other bioluminescent ostracods [28]. A
256 subset of these individuals (9 males, 11 females) were dissected to confirm sex. We partitioned
257 the data into clusters using the KMeans clustering algorithm implemented in scikit-learn [51] in
258 Python 2.7 [52]. KMeans fits the data into k clusters, specified in the arguments, sorting each data
259 point into the cluster which has the minimum euclidean distance to the centroid of the cluster.
260 The value for k was originally specified as eight based on the five known stages of instar
261 development for related species of ostracods plus the embryonic stage and adult males and
262 females. However, a k-value of eight clusters resulted in a split of the inferred adult female
263 cluster into two clusters rather than the discrimination of adult males from inferred A-I instars. To
264 avoid this apparent over-clustering, we ran our final analysis with a k-value of seven, which
265 retained all inferred adult females in a single cluster but was unable to distinguish an adult male

266 cluster from the inferred A-I instars. We assigned development stages to each cluster based on
267 the relationship by comparison to the closely related *Photeros annecohenae*, which grew in 12-
268 well dishes to allow more precise documentation of instars [28]. We further split the A-I
269 instar/Adult male cluster using the KMeans algorithm and a k-value of 3 with more precise
270 measurements of length, height, and eye width, as well as eye to keel distance (EKD) from an
271 additional sample of individuals that fell within this cluster (Sample size = 43). The three new
272 clusters were then assigned to development stages by comparing eye size and shape
273 parameters with what we expect based on *Photeros annecohenae* [28].
274
275 *Whole genome sequencing*
276 We froze four adult female *Vargula tsujii*, collected from the WMSC Dock on 2017-09-01 in
277 liquid nitrogen and shipped the specimens on dry-ice to the Hudson Alpha Institute for
278 Biotechnology Genomic Services Lab (HAIB-GSL) for genomic DNA extraction and Chromium
279 v2 Illumina sequencing library preparation. HAIB-GSL extracted the DNA using the Qiagen
280 MagAttract Kit, yielding 141 ng, 99 ng ,153 ng , and 96 ng of extracted DNA respectively. This
281 quantity of DNA was not sufficient for a size distribution analysis via agarose pulse field gel
282 analysis, therefore we decided to proceed with Chromium v2 library prep with the 153 ng
283 sample (sample # 5047), without confirmation of a suitable high-molecular weight DNA size
284 distribution. We sequenced this library on three lanes of a HiSeqX instrument using a 151x151
285 paired-end sequencing mode, resulting in a total of 910,926,987 paired reads (260.6 Gbp). We
286 attempted whole genome assembly of the resulting sequencing data with the Supernova v2.0.0
287 genome assembly software [53]. We then used the Agilent Femto Pulse High Molecular Weight
288 DNA capillary electrophoresis instrument at the MIT BioMicro Center to perform a post
289 sequencing analysis of the size distribution of the DNA used for Chromium library preparation.
290
291

292 *Mitochondrial genome assembly*

293 To achieve a full length mitochondrial genome (mtDNA) assembly of *V. tsujii*, we partitioned and
294 assembled sequences separately from the nuclear genome. We mapped Illumina reads from
295 our Chromium libraries (Table S3) to the known mtDNA of the closest available relative, *Vargula*
296 *hilgendorfii* (NC_005306.1) [54] using bowtie2 (v2.3.3.1) [55] (parameters: --very-sensitive-local).
297 We then extracted read pairs with at least one read mapped from the resulting BAM file with
298 samtools (parameters: view -G 12), then name-sorted, extracted in FASTQ format (parameters:
299 samtools fastq) and input the reads into SPAdes (v3.11.1) [56] for assembly (parameters: --only-
300 assembler -k55,127). Inspection of the resulting assembly graph using Bandage (v.0.8.1) [57],
301 combined with a heuristic manual deletion of low coverage nodes (deletion of nodes with
302 coverage <200x, mean coverage ~250x) gave rise to two loops with sequence similarity to the
303 *V. hilgendorfii* mtDNA that both circularized through a single path (Supplementary Figure S1).
304 We then manually inspected this graph via a blastn (2.7.1+) [58] aligned against the *V. hilgendorfii*
305 mtDNA through SequenceServer (v1.0.11) [59] and visualized with the Integrated Genomics
306 Viewer (v2.4.5) [60]. We noted that the single circularizing path was homologous to the two
307 duplicated control regions reported in the *V. hilgendorfii* mtDNA [54]. We surmised that this
308 assembly graph structure indicated the *V. tsujii* mtDNA had the same global structure as the *V.*
309 *hilgendorfii* mtDNA, and so used the Bandage "specify exact path" tool to traverse the SPAdes
310 assembly graph and generate a FASTA file representing the circularized *V. tsujii* mtDNA with
311 the putative duplicated control regions (Figure S1). To avoid splitting sequence features across
312 the mtDNA circular sequence break, we circularly rotated this full assembly with the seqkit
313 (v0.7.2) [54,61] "restart" command, to set the first nucleotide of the FASTA file at the start codon of
314 ND2. We then confirmed 100% of the nucleotides via bowtie2 re-mapping of reads and
315 polishing with Pilon (v1.21) [62] (parameters: --fix all). We annotated the final assembly of the
316 mitochondrial genome using the MITOS2 web server [63] with the invertebrate mitochondrial

317 genetic code (translation table 5). We manually removed low confidence and duplicate gene
318 predictions from the MITOS2 annotation.
319
320 **Results**
321 *Population genetics analyses*
322 Our COI haplotype network revealed minimal structure among *V. tsujii* populations in southern
323 California (Figure 3A). Haplotypes from San Pedro and Catalina Island overlap or diverge by
324 only one to three mutations. Haplotypes from San Diego individuals, although still very similar to
325 haplotypes from Catalina Island and San Pedro, differ by at least eight mutations and show no
326 overlap with haplotypes from other populations of *V. tsujii*. However, the haplotype network for
327 16S indicates that sequences from San Diego individuals are identical to some individuals from
328 the other two populations (Figure 3B). Furthermore, although the model with three clusters was
329 favored in the DAPC analysis for each gene (Supplementary Figures S2 and S3), membership
330 in five of the six clusters includes individuals from different populations (Supplementary Figures
331 S4 and S5). Therefore our analyses do not support three genetically distinct populations as
332 defined by location.
333

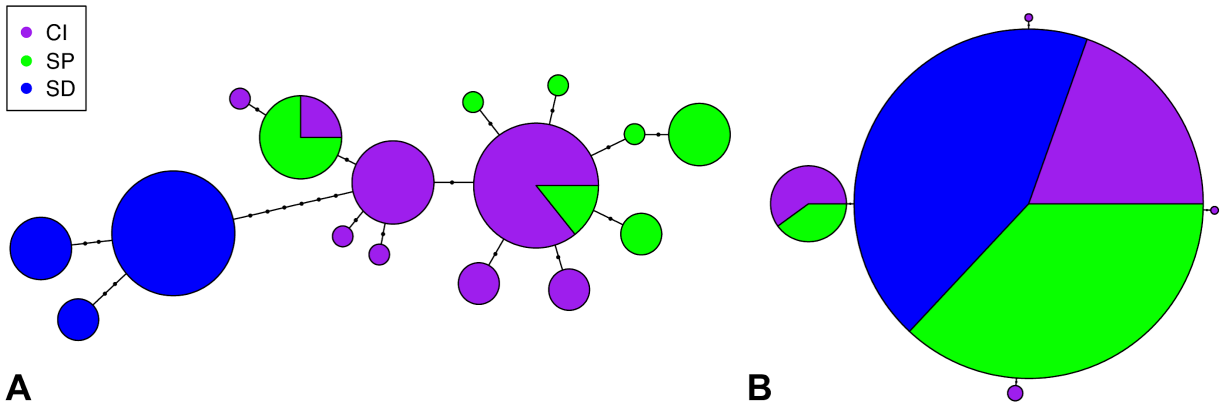

334
335 **Figure 3.** Haplotype networks for (A) COI sequences, and (B) 16S sequences of Vargula tsujii animals from three localities sampled. Abbreviations: CI, Catalina Island; SD, San Diego; SP, San Pedro.
336

Embryogenesis Description

After fertilization and release into the marsupium, *V. tsujii* embryos resemble opaque, green, ovoidal embryos (Figures 4 and 5). After five to eight days of growth, separation of the yolk begins, which appears as a light green mass condensed within the embryo. Around ten to eighteen days after deposition into the brooding chamber, two very small red lateral eyespots are visible on each embryo and the separation of the yolk continues. Daily observations over the next six days showed continual growth and darkening of the eyes. By day sixteen the yolk is almost completely separated and has begun to form the gut of the ostracod. By days fifteen to nineteen, the eyespots are mostly black and the light organ (a light brown/yellow mass) appears anteroventral to the eyes of the embryo. Around twenty days after deposition, developing limbs in the form of two rows of small brown masses are visible along the ventral side of the embryos. At this point the gut has finished forming within the carapace and is visible as a yellow-white mass on the posterior end of each embryo. Limb formation continues over the next few days, and the eyes of each embryo become entirely black. Twenty-five to thirty-eight days following embryo deposition, embryogenesis is complete, and instars are released from the mother's marsupium.

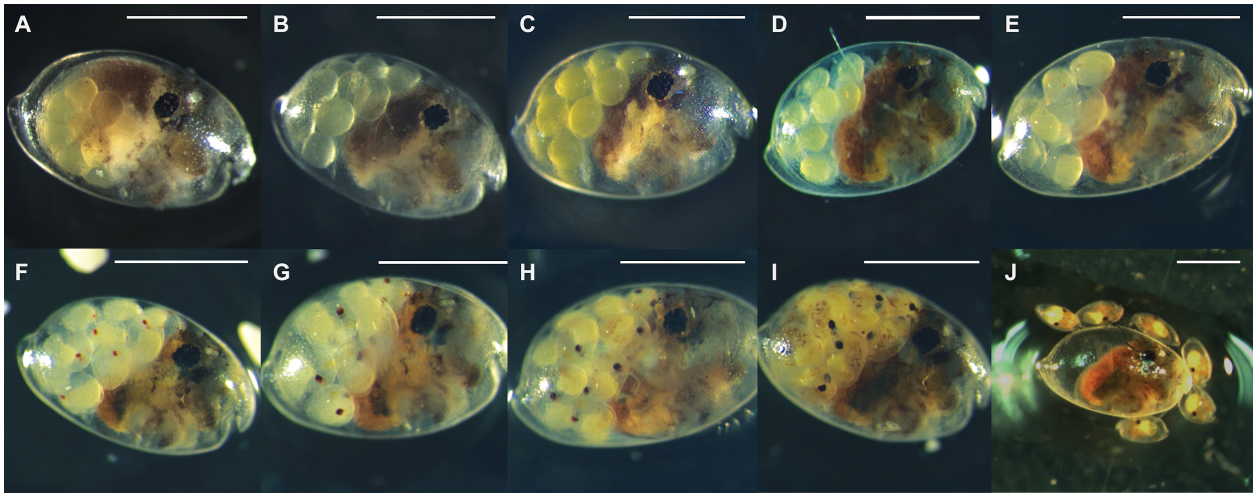

Figure 4. Embryogenesis within brooding females of V. tsujii post release into the marsupium. (A) Day 0, (B) Day 1-4, (C) Day 5-7, (D) Day 8-9, (E) Day 10-13, (F) Day 14-17, (G) Day 18-19, (H) Day 20-21, (I) Day 22-23, (J) Day 25-39.

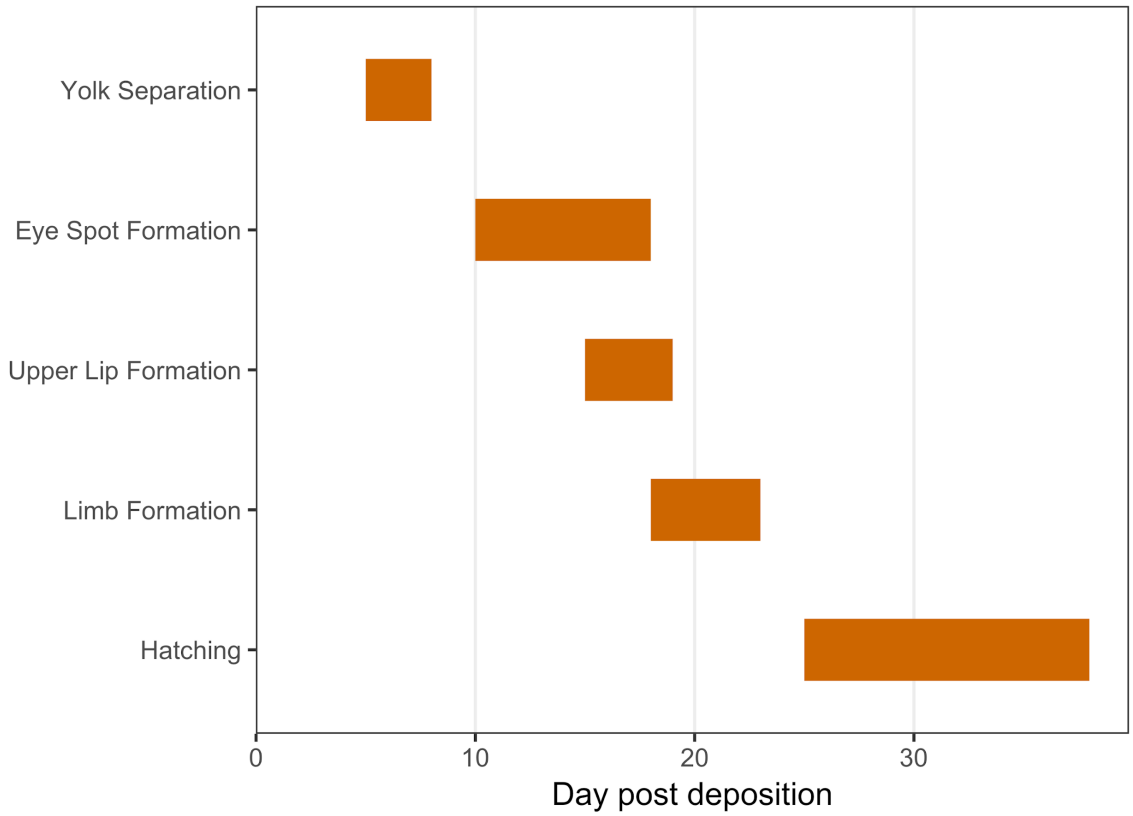

Figure 5. Summary of the timing of embryogenesis stages in V. tsujii. This represents the complete range of first appearance of each features across multiple broods, including: yolk separation (range = 5-8 days, N = 7); eye spot formation (range = 10-18 days, N = 12); upper lip formation (range = 15-19 days, N = 3); limb formation (range = 18-23 days, N = 11); hatching (range = 25-38 days, N = 11).

Instar development

We inferred five juvenile instar stages (A-I, A-II, A-III, A-IV, A-V) and an adult stage for Vargula tsujii (Figures 6, 7A; Table 2). Laboratory measurements of specimens of unknown sex were compared with the measurements of sexed individuals (9 males, 11 females) to confirm interpretation of the instar stage of size classes (Figure 7C-D). Due to large amounts of overlap of A-I females with adult and A-I males, these three groups are currently indistinguishable in the large data set. However, when we attempted to distinguish these stages using additional measurements (particularly eye-to-keel distance, EKD), we find that EKD differentiates A-I males and females, and that length separates the A-I instars from adult males (Figures 6E-G, 8; Table 3). Sexual dimorphism in size becomes apparent in adulthood, with adult females clearly

larger than adult males. However, compared to many other cypridinid ostracods, this dimorphism can be difficult to assess visually without a side-by-side comparison.

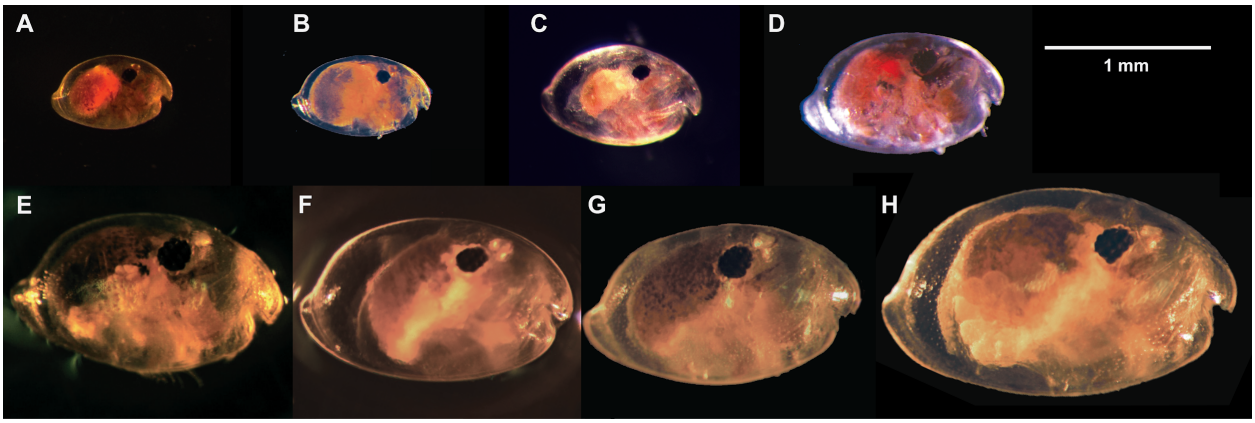

Figure 6. Images of selected individuals within each inferred instar stage: (A) A-V, (B) A-IV, (C) A-III, (D) A-II, (E) A-I male, (F) A-I female, (G) Adult male, (H) Adult female.

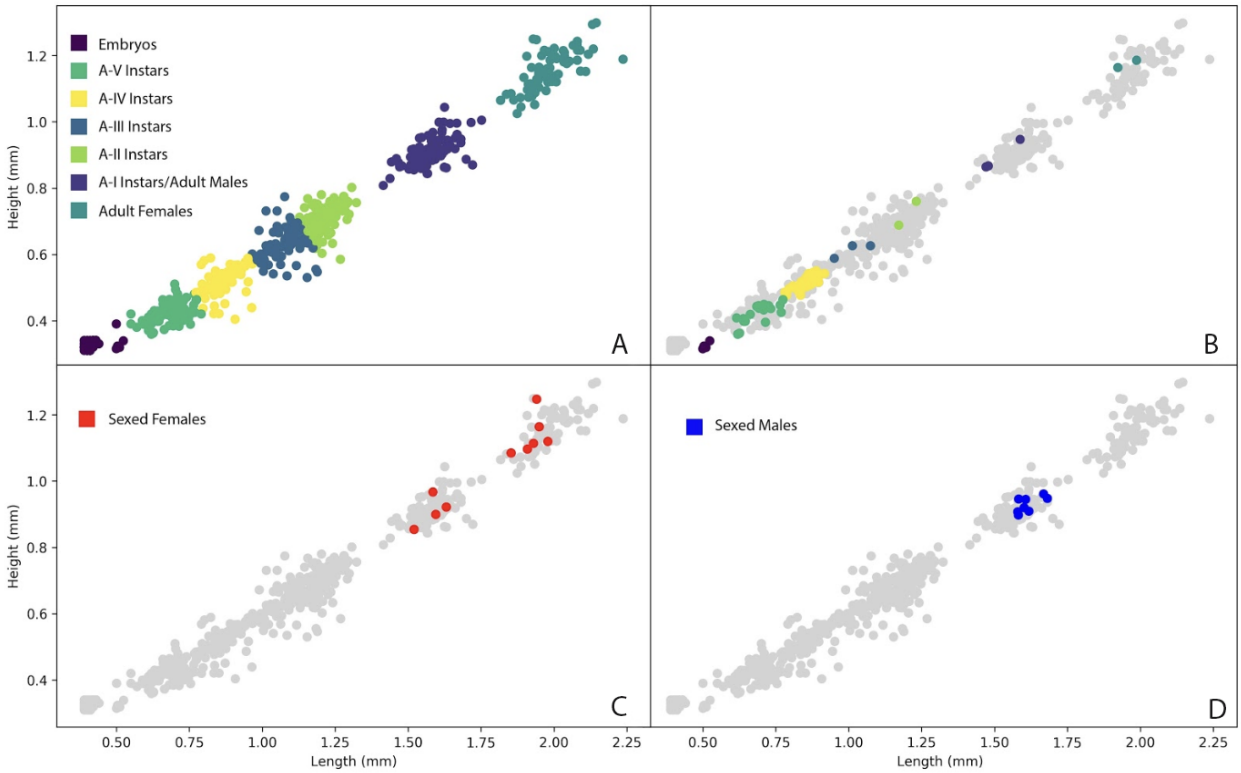

Figure 7. (A) K-means clusters of Vargula tsujii developmental stages based on carapace height and width. Instar stages were assigned to each cluster via comparison to P. annecohenae and additional analysis of male and female size dimorphism. (B) Points representing laboratory cultured animals overlayed on wild caught and unknown data. Different colors represent different clusters in the k-means analysis, and are labeled with their inferred instar/adult stages. (C) Shows wild-caught animals dissected and identified as female in relation to the k-means clusters, and (D) shows wild-caught animals dissected and identified as male in relation to the k-means clusters.

376 **Table 2.** Measurements for each cluster (and inferred instar) of *Vargula tsujii* ± SD.

Instar	**N**	**Carapace Length (mm) ± SD**	**Carapace Height (mm) ± SD**	**Eye width (mm) ± SD**
Embryo	84	0.418 ± 0.0271	0.326 ± 0.0112	0.0630 ± 0.0112
A-V	106	0.687 ± 0.0504	0.427 ± 0.0289	0.0682 ± 0.0164
A-IV	89	0.863 ± 0.0448	0.517 ± 0.0374	0.0684 ± 0.0271
A-III	66	1.078 ± 0.0516	0.632 ± 0.0494	0.121 ± 0.0208
A-II	96	1.214 ± 0.0426	0.711 ± 0.0409	0.133 ± 0.0160
Male A-I/Female A-I/ Adult Male	106	1.581 ± 0.0605	0.913 ± 0.0402	0.226 ± 0.0345
Adult Female	70	1.983 ± 0.0798	1.154 ± 0.0591	0.210 ± 0.0326

377

378 **Table 3.** Additional measurements for further inferring A-I Male, A-I Female, and Adult Male

379 instars, including length, height, eye width, and eye to keel distance (EKD) ± SD.

Inferred Instar	N	Length	Height	Eye size	EKD
A-I Male	15	1.566 ± 0.032	0.907 ± 0.039	0.218 ± 0.028	0.828 ± 0.053
A-I Female	15	1.592 ± 0.026	0.902 ± 0.030	0.198 ± 0.018	0.974 ± 0.038
Adult Male	13	1.647 ± 0.028	0.963 ± 0.023	0.242 ± 0.019	0.878 ± 0.040

380

381

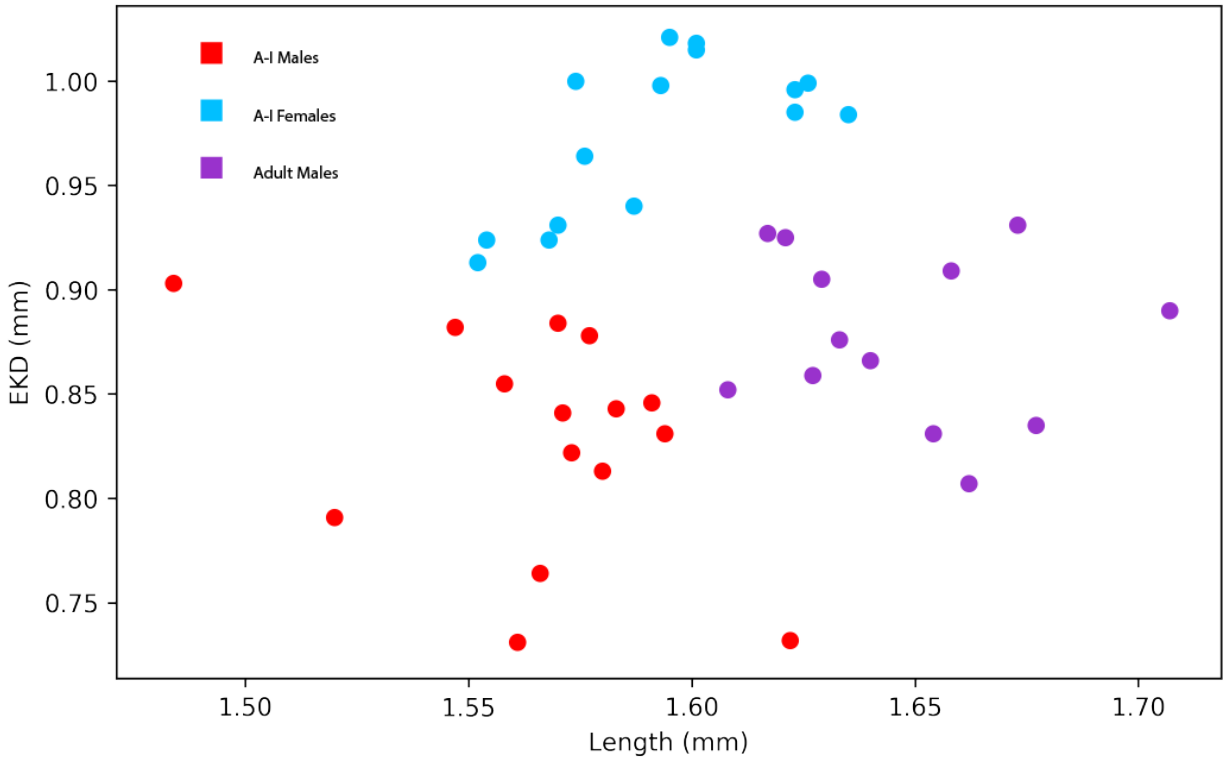

Figure 8. Plot of length versus eye to keel distance (EKD) in animals assigned to the A-I Instar/Adult Male cluster in the previous KMeans analysis (Figure 7A). These points were then clustered via KMeans analysis into three clusters, which we assigned to A-I Males (red), A-I Females (blue), and Adult Males (yellow).

Evidence for complete life cycle in the lab

To assess whether a complete life cycle was obtained in the laboratory, we began with only brooding females in a small experimental aquarium. Those brooding females, although not tracked individually, released a number of juveniles, which we measured intermittently over time (Figure 6B). In this aquarium we found juveniles, and eventually adults, that fell across the full size range of wild-caught ostracods. After all of the broods hatched, we removed all adult females from the experimental aquarium to assess whether the ostracods would mature and mate in the laboratory. Following removal of the original adult females, we found adult brooding females that grew up in experimental aquarium that themselves gave birth to the next generation in 3-4 months time.

394 *Nuclear and mitochondrial genome assemblies*

395 Our final *Vargula tsujii* nuclear genome assembly is highly fragmented, with an indication of high
396 levels of heterozygosity between haplotypes (~5%) and a high proportion of simple sequence
397 repeats. Our post-sequencing analysis indicated the mode of the DNA size distribution for the
398 four extracted DNA samples were 1244 bp, 3820 bp, 1285 bp (sample #5047), and 1279 bp,
399 respectively, with a tail of ~20-40 kbp in each sample.

400

401 The final *V. tsujii* mtDNA (15,729 bp) (Figure 9) aligned to the previously published *V.*
402 *hilgendorfii* mtDNA with 98% coverage and 78.5% nucleotide identity, and is available on NCBI
403 GenBank (MG767172). The *V. tsujii* mtDNA contains 22 tRNA genes, 13 protein coding genes,
404 and 2 duplicated control regions in an identical positioning and orientation to the *V. hilgendorfii*
405 mtDNA. The V. tsujii duplicate control regions (661 bp, 570 bp), are smaller than the
406 homologous V. hilgendorfii control regions (855 bp, 778 bp). The alignment of the V. tsujii
407 control regions to the V. hilgendorfii control regions indicate they possess reasonable nucleotide
408 identity (~73%), but the presence of unalignable regions ~20% of the length of the regions
409 suggests evolution constrained by size and/or GC% content rather than sequence identity
410 alone. There is one polymorphic base in the final mitogenome assembly coding for a
411 synonymous wobble mutation in the COII gene (COII:L76).

412

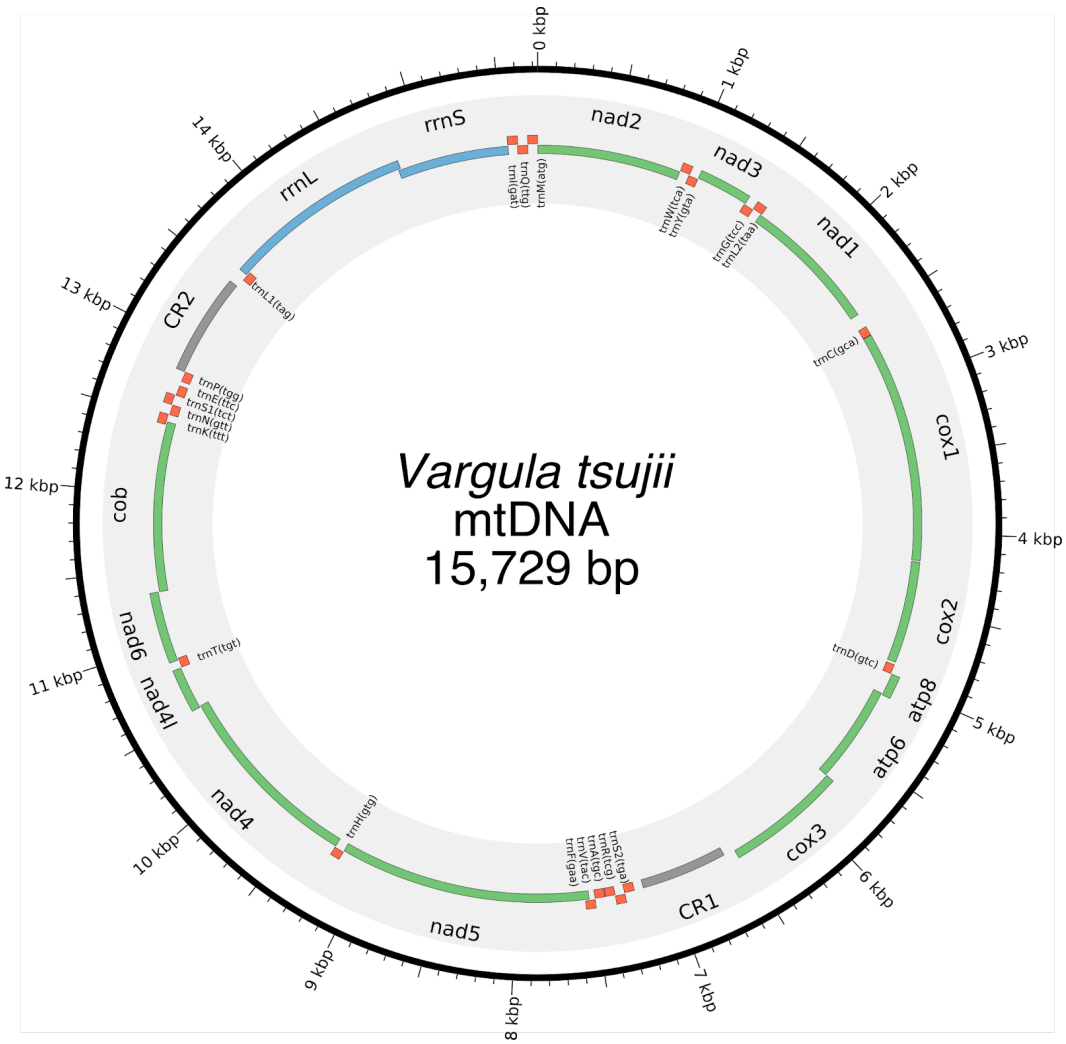

Figure 9. Mitochondrial genome of V. tsujii. Note the duplicated control regions, CR1 and CR2 (in gray). Figure produced with Circos.

Discussion

Based on measurement data on the first and second generations of ostracods reared in the lab (Figure 5), and the presence of brooding female ostracods in our experimental aquarium where adult females had previously been removed, we can infer that we were successful in rearing *Vargula tsujii* through its complete life cycle in the lab. This is a first for any bioluminescent ostracod, as rearing in the lab has remained a significant hurdle for laboratory studies in these animals [28,29]. However, despite recent improvements, challenges still remain. Recent improvements include adding a neoprene gasket to the edge of the false bottom to prevent sand

424 and detritus from falling below and fouling the aquarium and periodically siphoning the surface
425 of the sand in the aquarium to reduce build-up of detritus and fouling microorganisms. But
426 previous challenges mean our current population of animals is relatively small (between 500
427 and 1000 individuals), and we do not yet know if it is possible to continue the culture indefinitely
428 without new input of animals. Currently, we input new wild-caught animals about every 6
429 months to increase the population size. Furthermore, the populations within condos were very
430 prone to collapse, and animals do not survive long in 12-well dishes as they did in P.
431 annecohenae [28], limiting current experimental work.
432
433 Our current population was cultured from animals collected near Wrigley Marine Science Center
434 on Santa Catalina Island, which appears to contain much of the genetic diversity sampled
435 across much of the known the range of *V. tsujii* (Figure 3). Our population genetics analyses
436 support the hypothesis that populations of *Vargula tsujii* experience some gene flow across the
437 localities sampled, including Catalina Island. These results are consistent with the hypothesis
438 that *V. tsujii* represents a single, connected species. As such, we assume our culture of
439 ostracods from Santa Catalina Island, and inferences made from it, may be representative of
440 the genetic diversity of populations of *V. tsujii* across southern California coastal systems.
441 However, we cannot discount the possibility that there might be some variation in development
442 times and instar sizes across the range of this species. Also of note is that this species is not
443 easily collected throughout the reported range, and northern populations, if they exist, may be
444 divergent from southern California populations.
445
446 *Attempted whole genome reconstruction*
447 The 1C genome size of *Vargula tsujii* was previously reported to be 4.46 ± 0.08 pg (Female,
448 n=3), and 4.05 pg (Male, n=1) [64], corresponding to a 1C genome size of 4.36 Gbp and 3.96 Gbp
449 respectively and suggesting XO sex determination. Our reconstruction of the *Vargula tsujii*

450 nuclear genome assembly is highly fragmented, with an indication of high levels of
451 heterozygosity between haplotypes (~5%) and a high proportion of simple sequence repeats.
452 We speculate that our poor nuclear genome assembly results are likely due to the small size
453 distribution of the input DNA, as larger fragment sizes are especially critical for the
454 reconstruction of large genomes such as *V. tsujii*. Further protocol development is needed to
455 extract suitable High Molecular Weight DNA, which could allow long-read sequencing that would
456 improve assembly.
457
458 *The life cycle of* Vargula tsujii
459 The embryogenesis of *Vargula tsujii* is similar to closely related species, and the 24-day
460 average brooding duration falls within the range for other cypridinid ostracods (10-30 days) [65].
461 The primary stages of *V. tsujii* late-stage embryogenesis are yolk separation, formation of eye
462 spots, development of the upper lip, development of limbs, and emergence from the chorion and
463 marsupium (Figure 5). In general, the late-stage embryonic development of *Vargula tsujii* is
464 longer than that of other luminescent ostracods whose development has been described (Table
465 4). Longer overall development in the temperate V. tsujii is consistent with work in other
466 crustaceans, which indicates that temperature has an inverse relationship with development
467 time [66]. However, earlier embryonic development in *V. tsujii* is faster than in the tropical *P.*
468 *annecohenae*. In *P. anncohenae,* yolk separation begins on day 9 and eye development begins
469 on days 14-15 [28], while those stages begin at 5-7 and 10-13 days, respectively, in *V. tsujii*.
470 Additionally, the order of development in *V. tsujii* appears to differ from that of *Vargula*
471 *hilgendorfii,* which starts to develop limbs on days 4-5, before eye and upper lip development [67].
472 By contrast, *V. tsujii* limbs do not appear until after eye-spot and upper lip formation. The
473 reasons for this difference are unclear.
474

475 **Table 4**. Comparison of embryogenesis timing between five different ostracod species post-

476 deposition. Species with an asterisk (*) are bioluminescent cypridinids.

Species	Cloudy Embryo	Yolk Sep.	Eye Spot Formation	Upper Lip	Limbs	Release	Citation
*Vargula tsujii** *(Myodocopida: Cypridinidae)*	3-4 days	5-8 days	10-18 days	15-19 days	18-23 days	25-38 days	This study
Photeros *annecohenae** *(Myodocopida: Cypridinidae)*	2-3 days	9 days	14-15 days	17 days	-	19 days	[28]
*Vargula hilgendorfii** (Myodocopida: Cypridinidae)	-	1-2 Days	6-8 days	6-8 days	4-5 days	16 days	[29]
Euphilomedes carcharodonta (Myodocopida: Philomedidae)	-	14 days	58-70 days	-	14-41 days	65-75 days	[31]
Xestoleberis hanaii (Podocopida: Xestoleberididae)	-	-	-	-	-	9-11 days	[34]

477

478 Juvenile development of *Vargula tsujii* is also quite similar overall to that of *Photeros*

479 *annecohenae*, the only other bioluminescent cypridinid ostracod for which instar developmental

480 data are available [28]. We inferred five distinct instar stages (A-V through A-I), and A-I instars

481 develop into size dimorphic adult males and females (Tables 2 and 3). It is important to note

482 that these inferences represent hypotheses that can be tested by rearing and measuring

483 individuals through molts, which we have not yet been able to accomplish in our culture.

484 However, average measurements of size, including carapace length and height, as well as eye

485 width, were comparable between respective instar stages in *V. tsujii* (inferred) and *P.*

486 *annecohenae* (observed). However, in *V. tsujii* average eye width remains within the range of

487 0.060 mm to 0.0684 mm from the embryonic stage until the second instar, and makes a large

488 jump by about two fold in the third instar (0.121 ± 0.0208 mm), as compared to a gradual
489 increase in eye size in *P. annecohenae*. In our KMeans clustering analysis, the second-to-
490 largest cluster of *V. tsujii* appears to contain adult males as well as A-I males and females. This
491 finding differs from that in *P. annecohenae*, where adult males were found to cluster separately
492 from A-I males and females and adult females based on size and shape, and A-I males and
493 females could be distinguished by certain shape parameters, as well as eye size [28]. In V. tsujii,
494 A-I males and females appear to be differentiated largely by eye-to-keel distance, which was not
495 measured in previous studies [28], and adult males can be separated from A-I instars by length
496 (Figure 8; Table 3). We hypothesize that this apparent reduction of sexual dimorphism observed
497 in the later stages of development, compared to *P. annecohenae*, may occur because *V. tsujii*
498 may have lost the ability to use luminescence for courtship [23], so selection acting on differences
499 in male and female shape may have been reduced.
500
501 *Benefits of completing the life cycle*
502 Cypridinid ostracods represent an independent origin of endogenous autogenic
503 bioluminescence. This group is a natural comparison to other, well-studied bioluminescent
504 courtship systems, such as that of fireflies [68]. Other possible laboratory models for
505 bioluminescence, such as brittle stars [69] and cnidarians [70] are useful for some research tasks,
506 such as studies of luciferins obtained from the diet (e.g., coelenterazine). Others might be easier
507 to rear in the laboratory, such as the self-fertilizing brittle star *Amphiolus squamata* [71]. However,
508 ostracods produce their own luciferase and luciferin, unlike brittle stars and cnidarians.
509 Ostracods also have relatively fast generation times (on the order of months), which can be
510 modified somewhat by adjusting the temperature of the water, as is common among ostracods
511 [27–29,72,73]. In comparison, fireflies are usually on a six-month to one-year life cycle that is difficult
512 to alter [74–76], and some brittle stars appear to spawn only seasonally [77,78]. Furthermore, culture
513 of an organism (*Vargula tsujii*) from a clade with an independent origin of autogenic

514 bioluminescence allows for comparative studies between luminescence in ostracods and the
515 autogenic bioluminescence found in fireflies [16] or other organisms, which would not otherwise
516 be possible.
517
518 Ostracods will be incredibly useful for studying the physiology and biochemistry of
519 bioluminescence [2,16], as both diversification and behavioral changes in cypridinids related to
520 luminescence have occurred using the same luciferin and homologous luciferases [25].
521 Furthermore, although Vargula tsujii itself does not possess bioluminescent signaling, we expect
522 a similar culturing system could be useful for some signaling species as well, at least those that
523 come to baited traps. Given that ostracod courtship signals may be simulated in a laboratory
524 setting, this system could allow us to assess male and female behavior in response to changes
525 in signal parameters, such as intensity, color, and pulse duration [79]. These tools will provide
526 researchers with an excellent system for asking important questions related to selection on
527 genes important for rapid diversification [80], including those related to behavior [81], sexual
528 selection [82], and the role of the biochemical properties of bioluminescence [26].
529
530 Importantly, the biosynthetic pathway for luciferin production is currently unknown for any
531 animal. One major obstacle to describing this pathway has been building laboratory cultures for
532 animal species that produce luciferin themselves and also have a relatively fast generation time.
533 Solving this bottleneck to accessing specimens for bioluminescent ostracods has set the stage
534 for investigations into the biosynthetic pathway of cypridinid luciferin and its possible use in
535 biomedical tools such as optogenetics [83]. Finally, this is an excellent system with which to
536 consider developing genome editing techniques (e.g., CRISPR/Cas9) [84] to test candidate genes
537 for luciferin biosynthesis and to assess how genetic variants in critical genes might affect
538 production or perception of bioluminescent signals.
539

Acknowledgements

We thank the USC *Wrigley Institute* for *Environmental Studies* for transportation and use of the facilities at the Wrigley Marine Science Center on Catalina Island, CA. JDM worked on the project at Wrigley during the Catalina Marine Biology Semester hosted by California State University and with support from the NSF (Award DEB·1457462 to ET). JAG was supported by the NSF (PRFB Award: 1711201). Population genetic work was supported by a mini-grant from Cal State LA to ET; sequence data were obtained from the Masters thesis of KH Lee; DM Jacinto and E Stiner helped with collections throughout California; RM Serrano helped with measurements of some specimens; N Hensley contributed data on collecting locations. Genomic sequencing was supported by the Beckman Young Investigator Award to JKW from the Arnold and Mabel Beckman Foundation and by a UCSB Faculty Seed Grant to THO. Finally, we would like to thank Simone Brandão and two anonymous reviewers for their comments on our manuscript.

Author contributions

JAG, ET, JKW, and THO conceived of and designed the study; JAG, GM, MNB, MSD, JDM, TRF, and DTS contributed to the acquisition and analysis of the data in this study; all authors participated in the interpretation of data, helped draft or substantially revise the manuscript, and gave final approval for publication.

Competing interests

The authors declare no competing interests.

Data availability

Sequence data for COI and 16S are available in GenBank (Table S1) and our whole genome Chromium reads are available in the Sequence Read Archive (SRR9308458). Scripts and data

566 for the population genetics and k-means clustering analyses are provided on Github
567 (https://github.com/goodgodric28/vargula_tsujii_culture). An additional video which shows
568 *Vargula tsujii* hatching from the chorion and outside the mother is provided on Youtube
569 (https://youtu.be/8o5CqHTcTjI).
570

571 **References**

572 1. Haddock, S. H. D., Moline, M. A. & Case, J. F. Bioluminescence in the sea. *Ann. Rev.*
573 *Mar. Sci.* **2**, 443–493 (2010).
574 2. Hastings, J. W. Biological diversity, chemical mechanisms, and the evolutionary origins
575 of bioluminescent systems. *J. Mol. Evol.* **19**, 309–321 (1983).
576 3. Shimomura, O., Johnson, F. H. & Saiga, Y. Extraction, purification and properties of
577 aequorin, a bioluminescent protein from the luminous hydromedusan, *Aequorea*. *J. Cell.*
578 *Comp. Physiol.* **59**, 223–239 (1962).
579 4. Tsuji, F. I. ATP-dependent bioluminescence in the firefly squid, *Watasenia scintillans*.
580 *Proc. Natl. Acad. Sci. U. S. A.* **82**, 4629–4632 (1985).
581 5. Cormier, M. J., Wampler, J. E., Hori, K. & Lee, J. W. Bioluminescence of *Renilla*
582 *reniformis*. IX. Structured bioluminescence. Two emitters during both the in vitro and the
583 in vivo bioluminescence of the sea pansy, *Renilla*. *Biochemistry* **10**, 2903–2909 (1971).
584 6. Dunlap, P. Biochemistry and Genetics of Bacterial Bioluminescence. in *Advances in*
585 *Biochemical Engineering/Biotechnology* 37–64 (2014).
586 7. Fallon, T. R. *et al.* Firefly genomes illuminate parallel origins of bioluminescence in
587 beetles. *Elife* **7**, (2018).
588 8. Sweeney, B. The bioluminescence of dinoflagellates. in *Biochemistry and Physiology of*
589 *Protozoa* 287–306 (1979).
590 9. Kobayashi, K. *et al.* Purification and properties of the luciferase from the marine ostracod
591 *Vargula hilgendorfii*. in *Bioluminescence and Chemiluminescence* (2001).

592 doi:10.1142/9789812811158_0022.

593 10. Hastings, J. W., Vergin, M. & Desa, R. Scintillons: The Biochemistry of Dinoflagellate
594 Bioluminescence. in *Bioluminescence in Progress* 301–330 (Princeton University Press,
595 1967).

596 11. Nakatsu, T. *et al.* Structural basis for the spectral difference in luciferase
597 bioluminescence. *Nature* **440**, 372–376 (2006).

598 12. Marques, S. M. & Esteves da Silva, J. C. G. Firefly bioluminescence: a mechanistic
599 approach of luciferase catalyzed reactions. *IUBMB Life* **61**, 6–17 (2009).

600 13. Verhaegent, M. & Christopoulos, T. K. Recombinant *Gaussia* luciferase.
601 Overexpression, purification, and analytical application of a bioluminescent reporter for
602 DNA hybridization. *Anal. Chem.* **74**, 4378–4385 (2002).

603 14. Dunlap, P. V. & Urbanczyk, H. Luminous Bacteria. in *The Prokaryotes* (ed. Rosenberg
604 E., DeLong E.F., Lory S., Stackebrandt E., Thompson F.) 495–528 (Springer, 2013).

605 15. Kotlobay, A. A. *et al.* Genetically encodable bioluminescent system from fungi. *Proc.*
606 *Natl. Acad. Sci. U. S. A.* **115**, 12728–12732 (2018).

607 16. Kanie, S., Nakai, R., Ojika, M. & Oba, Y. 2-S-cysteinylhydroquinone is an intermediate
608 for the firefly luciferin biosynthesis that occurs in the pupal stage of the Japanese firefly,
609 *Luciola lateralis*. *Bioorg. Chem.* **80**, 223–229 (2018).

610 17. McLean, M., Buck, J. & Hanson, F. E. Culture and larval behavior of photurid fireflies.
611 *Am. Midl. Nat.* **87**, 133 (1972).

612 18. Thompson, E. M., Nagata, S. & Tsuji, F. I. Cloning and expression of cDNA for the
613 luciferase from the marine ostracod *Vargula hilgendorfii*. *Proc. Natl. Acad. Sci. U. S. A.*
614 **86**, 6567–6571 (1989).

615 19. Oba, Y., Kato, S.-I., Ojika, M. & Inouye, S. Biosynthesis of luciferin in the sea firefly,
616 *Cypridina hilgendorfii*: l-tryptophan is a component in *Cypridina* luciferin. *Tetrahedron*
617 *Lett.* **43**, 2389–2392 (2002).

20. de Wet, J. R., Wood, K. V., Helinski, D. R. & DeLuca, M. Cloning of firefly luciferase cDNA and the expression of active luciferase in *Escherichia coli*. *Proc. Natl. Acad. Sci. U. S. A.* **82**, 7870–7873 (1985).

21. Seliger, H. H., McElroy, W. D., White, E. H. & Field, G. F. Stereo-specificity and firefly bioluminescence, a comparison of natural and synthetic luciferins. *Proc. Natl. Acad. Sci. U. S. A.* **47**, 1129–1134 (1961).

22. Brandão, S. N., Angel, M. V., Karanovic, I., Perrier, V. & Meidla, T. World Ostracoda Database. http://www.marinespecies.org/ostracoda (2019) doi:10.14284/364.

23. Cohen, A. C. & Morin, J. G. Sexual morphology, reproduction and the evolution of bioluminescence in Ostracoda. *Paleontological Society Papers* **9**, 37 (2003).

24. Ellis, E. A. & Oakley, T. H. High rates of species accumulation in animals with bioluminescent courtship displays. *Curr. Biol.* **26**, 1916–1921 (2016).

25. Morin, J. G. Based on a review of the data, use of the term 'cypridinid' solves the *Cypridina*/*Vargula* dilemma for naming the constituents of the luminescent system of ostracods in the family cypridinidae. *Luminescence* **26**, (2011).

26. Hensley, N. M. *et al.* Phenotypic evolution shaped by current enzyme function in the bioluminescent courtship signals of sea fireflies. *Proc. R. Soc. B* **286**, 20182621 (2019).

27. Cohen, A. C. Rearing and postembryonic development of the myodocopid ostracode *Skogsbergia lerneri* from coral reefs of Belize and the Bahamas. *J. Crustacean Biol.* **3**, 235–256 (1983).

28. Gerrish, G. A. & Morin, J. G. Life cycle of a bioluminescent marine ostracode, *Vargula annecohenae* (Myodocopida: Cypridinidae). *J. Crustacean Biol.* **28**, 669–674 (2008).

29. Wakayama, K & Kanazawa, K. Elucidation of environmental tolerance of sea fireflies and research on construction of optimal rearing environment *Sci. J. Kangawa U.* **25**, 117-124 (2014).

30. Pérez-Lloréns, J. L. Cooking-Science-Communication (CSC): The ideal trident to enjoy

the dining experience. *International Journal of Gastronomy and Food Science* **16**, 100134 (2019).

31. Koyama, K. H. & Rivera, A. S. Embryonic development of the myodocopid ostracod *Euphilomedes carcharodonta* Smith, 1952. *J. Crustacean Biol.* (2018) doi:10.1093/jcbiol/ruy088.

32. Kawamata, K., Sato, M. & Abe, K. Complete life cycle of the ostracod *Euphilomedes nipponica* (Myodocopida, Philomedidae). *Plankton Benthos Res.* **13**, 83–89 (2018).

33. Smith, R. J. & Kamiya, T. The Ontogeny of *Neonesidea oligodentata* (Bairdioidea, Ostracoda, Crustacea). *Hydrobiologia* **489**, 245–275 (2002).

34. Ikeya, N. & Kato, M. The life history and culturing of *Xestoleberis hanaii* (Crustacea, Ostracoda). in *Evolutionary Biology and Ecology of Ostracoda* (eds. Horne, D. J. & Martens, K.) 149–159 (Springer Netherlands, 2000).

35. Liberto, R., César, I. I. & Mesquita-Joanes, F. Postembryonic growth in two species of freshwater Ostracoda (Crustacea) shows a size-age sigmoid model fit and temperature effects on development time, but no clear temperature-size rule (TSR) pattern. *Limnology* **15**, 57–67 (2014).

36. Kubanç, N., Özuluğ, O. & Kubanç, C. The ontogeny of appendages of *Heterocypris salina* (Brady, 1868) Ostracoda (Crustacea). *Ostracodology — Linking Bio- and Geosciences* 255–272 (2007).

37. Smith, R. J. & Martens, K. The ontogeny of the cypridid ostracod *Eucypris virens* (Jurine, 1820) (Crustacea, Ostracoda). in *Evolutionary Biology and Ecology of Ostracoda* (eds. Horne, D. J. & Martens, K.) vol. 148 31–63 (Springer, 2000).

38. Engstrom, D. R. & Nelson, S. R. Paleosalinity from trace metals in fossil ostracodes compared with observational records at Devils Lake, North Dakota, USA. *Palaeogeography, Palaeoclimatology, Palaeoecology* **83**, 295–312 (1991).

39. Korniker, L. S. & Baker, J. H. *Vargula tsujii*, a new species of luminescent ostracod from

lower and southern California (Myodocopa: Cypridininae). *Proceedings of the Biological Society of Washington* **90**, 218–231 (1977).

40. Hammer, R. M. Day-night differences in the emergence of demersal zooplankton from a sand substrate in a kelp forest. *Mar. Biol.* **62**, 275–280 (1981).

41. Stepien, C. A. & Brusca, R. C. Nocturnal attacks on nearshore fishes in southern California by crustacean zooplankton. *Marine Ecology Progress Series* **25**, 91–105 (1985).

42. Warner, J. A. & Case, J. F. The zoogeography and dietary induction of bioluminescence in the midshipman fish, *Porichthys notatus*. *The Biological Bulletin* **159**, 231–246 (1980).

43. Cohen, A. C. & Oakley, T. H. Collecting and processing marine ostracods. *J. Crustacean Biol.* **37**, 347–352 (2017).

44. Lee, K. H.-H. Genetic differentiation in *Vargula tsujii* (Ostracoda: Cypridinidae) along the California coast. (California State University, Los Angeles, 2002).

45. Paradis, E. pegas: an R package for population genetics with an integrated-modular approach. *Bioinformatics* **26**, 419–420 (2010).

46. R Core Team. *R: A Language and Environment for Statistical Computing*. (R Foundation for Statistical Computing, 2019).

47. Jombart, T. adegenet: a R package for the multivariate analysis of genetic markers. *Bioinformatics* **24**, 1403–1405 (2008).

48. Schwarz, G. Estimating the Dimension of a Model. *The Annals of Statistics* **6**, 461–464 (1978).

49. Vannier, J., Abe, K. & Ikuta, K. Feeding in myodocopid ostracods: functional morphology and laboratory observations from videos. *Marine Biology* **132**, 391–408 (1998).

50. Schindelin, J. *et al.* Fiji: an open-source platform for biological-image analysis. *Nat. Methods* **9**, 676–682 (2012).

51. Garreta, R. & Moncecchi, G. *Learning scikit-learn: Machine learning in Python*. (Packt

696 Publishing Ltd, 2013).
697 52. van Rossum, G. *Python tutorial*, *Technical Report CS-R9526, Centrum voor Wiskunde*
698 *en Informatica (CWI)* (1995).
699 53. Weisenfeld, N. I., Kumar, V., Shah, P., Church, D. M. & Jaffe, D. B. Direct determination
700 of diploid genome sequences. *Genome Res.* **27**, 757–767 (2017).
701 54. Ogoh, K. & Ohmiya, Y. Complete mitochondrial DNA sequence of the sea-firefly,
702 *Vargula hilgendorfii* (Crustacea, Ostracoda) with duplicate control regions. *Gene* **327**,
703 131–139 (2004).
704 55. Langmead, B. & Salzberg, S. L. Fast gapped-read alignment with Bowtie 2. *Nat.*
705 *Methods* **9**, 357–359 (2012).
706 56. Nurk, S. *et al.* Assembling genomes and mini-metagenomes from highly chimeric reads.
707 *Lecture Notes in Computer Science* 158–170 (2013).
708 57. Wick, R. R., Schultz, M. B., Zobel, J. & Holt, K. E. Bandage: interactive visualization of
709 de novo genome assemblies. *Bioinformatics* **31**, 3350–3352 (2015).
710 58. Camacho, C. *et al.* BLAST+: architecture and applications. *BMC Bioinformatics* **10**, 421
711 (2009).
712 59. Priyam, A. *et al.* Sequenceserver: A modern graphical user interface for custom BLAST
713 databases. *Mol. Biol. Evol.* **36**, 2922–2924 (2019).
714 60. Robinson, J. T. *et al.* Integrative genomics viewer. *Nat. Biotechnol.* **29**, 24–26 (2011).
715 61. Shen, W., Le, S., Li, Y. & Hu, F. SeqKit: A cross-platform and ultrafast toolkit for
716 FASTA/Q file manipulation. *PLoS One* **11**, e0163962 (2016).
717 62. Walker, B. J. *et al.* Pilon: an integrated tool for comprehensive microbial variant
718 detection and genome assembly improvement. *PLoS One* **9**, e112963 (2014).
719 63. Bernt, M. *et al.* MITOS: Improved de novo metazoan mitochondrial genome annotation.
720 *Molecular Phylogenetics and Evolution* **69**, 313–319 (2013).
721 64. Jeffery, N. W., Ellis, E. A., Oakley, T. H. & Ryan Gregory, T. The genome sizes of

722 ostracod crustaceans correlate with body size and evolutionary history, but not
723 environment. *Journal of Heredity* **108**, 701–706 (2017).
724 65. Cohen, A. C. & Morin, J. G. Patterns of reproduction in ostracodes: A review. *Journal of*
725 *Crustacean Biology* **10**, 184 (1990).
726 66. Steele, D. H. & Steele, V. J. Egg size and duration of embryonic development in
727 Crustacea. *Internationale Revue der gesamten Hydrobiologie und Hydrographie* **60**,
728 711–715 (1975).
729 67. Wakayama, N. Embryonic development clarifies polyphyly in ostracod crustaceans.
730 *Journal of Zoology* **273**, 406–413 (2007).
731 68. Lewis, S. M. & Cratsley, C. K. Flash signal evolution, mate choice, and predation in
732 fireflies. *Annu. Rev. Entomol.* **53**, 293–321 (2008).
733 69. Deheyn, D. D. Bioluminescence in the brittle star *Amphiolis squamata* (Echinodermata):
734 an overview of 10 years of research. *Bioluminescence and Chemiluminescence* (2001)
735 doi:10.1142/9789812811158_0009.
736 70. Houliston, E., Momose, T. & Manuel, M. *Clytia hemisphaerica*: a jellyfish cousin joins the
737 laboratory. *Trends Genet.* **26**, 159–167 (2010).
738 71. Boissin, E., Hoareau, T. B., Féral, J. P. & Chenuil, A. Extreme selfing rates in the
739 cosmopolitan brittle star species complex *Amphipholis squamata*: data from progeny-
740 array and heterozygote deficiency. *Marine Ecology Progress Series* **361**, 151–159
741 (2008).
742 72. Heip, C. The life-cycle of *Cyprideis torosa* (Crustacea, Ostracoda). *Oecologia* **24**, 229–
743 245 (1976).
744 73. Martens, K. Effects of temperature and salinity on postembryonic growth in *Mytilocypris*
745 *henricae* (Chapman) (Crustacea, Ostracoda). *Journal of Crustacean Biology* **5**, 258–272
746 (1985).
747 74. Viviani, V. R. Fireflies (Coleoptera: Lampyridae) from southeastern Brazil: Habitats, life

748 history, and bioluminescence. *Ann. Entomol. Soc. Am.* **94**, 129–145 (2001).
749 75. Ho, J.-Z., Chiang, P.-H., Wu, C.-H. & Yang, P.-S. Life cycle of the aquatic firefly *Luciola*
750 *ficta* (Coleoptera: Lampyridae). *J. Asia. Pac. Entomol.* **13**, 189–196 (2010).
751 76. Fu, X., Nobuyoshi, O., Vencl, F. V. & Lei, C. Life cycle and behaviour of the aquatic
752 firefly *Luciola leii* (Coleoptera: Lampyridae) from mainland China. *The Canadian*
753 *Entomologist* **138**, 860–870 (2006).
754 77. Soong, K., Lin, Y., Chao, S. & Chang, D. Spawning time of two shallow-water brittle
755 stars. *Marine Ecology Progress Series* **376**, 165–171 (2009).
756 78. Hagman, D. K. & Vize, P. D. Mass spawning by two brittle star species, *Ophioderma*
757 *rubicundum* and *O. Squamosissimum* (Echinodermata: Ophiuroidea), at the Flower
758 Garden Banks, Gulf of Mexico. *Bull. Mar. Sci.* **72**, 871–876 (2003).
759 79. Rivers, T. J. & Morin, J. G. Female ostracods respond to and intercept artificial
760 conspecific male luminescent courtship displays. *Behavioral Ecology* **24**, 877–887
761 (2013).
762 80. Stern, D. L. & Orgogozo, V. Is genetic evolution predictable? *Science* **323**, 746–751
763 (2009).
764 81. Boake, C. R. B. *et al.* Genetic tools for studying adaptation and the evolution of behavior.
765 *Am. Nat.* **160 Suppl 6**, S143–59 (2002).
766 82. Ritchie, M. G. Sexual selection and speciation. *Annual Review of Ecology, Evolution,*
767 *and Systematics* **38**, 79–102 (2007).
768 83. Yeh, H.-W. & Ai, H.-W. Development and applications of bioluminescent and
769 chemiluminescent reporters and biosensors. *Annu. Rev. Anal. Chem.* **12**, 129–150
770 (2019).
771 84. Cong, L. *et al.* Multiplex genome engineering using CRISPR/Cas systems. *Science* **339**,
772 819–823 (2013).
773 85. Pang, K. & Martindale, M. Q. *Mnemiopsis leidyi* spawning and embryo collection. *CSH*

774 *Protoc.* **2008**, db.prot5085 (2008).
775 86. Warren, K. J. The establishment and characterization of primary cell cultures derived
776 from the ctenophore *Mnemiopsis leidyi*. (University of Miami, 2016).
777 87. Baker, L. D. & Reeve, M. R. Laboratory culture of the lobate ctenophore *Mnemiopsis*
778 *mccradyi* with notes on feeding and fecundity. *Marine Biology* **26**, 57–62 (1974).
779 88. Kahn, B. Scientists Have Cultivated a Mesmerizing Jelly That's Like 'Barely Organized
780 Water'. *Earther* https://earther.gizmodo.com/scientists-have-cultivated-a-mesmerizing-
781 jelly-thats-li-1823207295 (2018).
782 89. Lindner, A. & Migotto, A. E. The life cycle of *Clytia linearis* and *Clytia noliformis*:
783 metagenic campanulariids (Cnidaria: Hydrozoa) with contrasting polyp and medusa
784 stages. *Journal of the Marine Biological Association of the United Kingdom* **82**, 541–553
785 (2002).
786 90. Delroisse, J., Ortega-Martinez, O., Dupont, S., Mallefet, J. & Flammang, P. De novo
787 transcriptome of the European brittle star *Amphiura filiformis* pluteus larvae. *Mar.*
788 *Genomics* **23**, 109–121 (2015).
789 91. Oba, Y. *et al.* Bioluminescence of a firefly pupa: involvement of a luciferase isotype in
790 the dim glow of pupae and eggs in the Japanese firefly, Luciola lateralis. *Photochem.*
791 *Photobiol. Sci.* **12**, 854–863 (2013).
792 92. Watkins, O. C., Sharpe, M. L., Perry, N. B. & Krause, K. L. New Zealand glowworm
793 (*Arachnocampa luminosa*) bioluminescence is produced by a firefly-like luciferase but an
794 entirely new luciferin. *Sci. Rep.* **8**, 3278 (2018).
795 93. Meyer-Rochow, V. B. Glowworms: a review of *Arachnocampa* spp. and kin.
796 *Luminescence* **22**, 251–265 (2007).
797 94. Takaie, H. Ten years of the glow-worm (*Arachnocampa richardsae*) rearing at Tama
798 Zoo--Fascination of a living milky way. *Insectarium* **34**, 336–342 (1997).
799 95. Maheswarudu, G. & Vineetha, A. Culture of the littoral oligochaete *Pontodrilus*

bermudensis Beddard. *The Journal of Bioprocess Technology* **97**, 142–155 (2013).

96. Nishida, H. Development of the appendicularian *Oikopleura dioica*: culture, genome, and cell lineages. *Dev. Growth Differ.* **50 Suppl 1**, S239–56 (2008).

97. Martí-Solans, J. *et al. Oikopleura dioica* culturing made easy: a low-cost facility for an emerging animal model in EvoDevo. *Genesis* **53**, 183–193 (2015).

826

827 **Figures**

828 **Figure 1.** Map of localities where collections (and attempted collections) of *Vargula tsujii* were
829 made. Black points represent geographic annotations for reference, purple points refer to the
830 location where ostracods were collected that were ultimately cultured, blue where animals were
831 found or collected, orange where Kornicker originally collected animals, and red where no *V.*
832 *tsujii* were found. (A) Map of the California (USA) coastline where collections were attempted;
833 (B) Map of the region near Two Harbors (Santa Catalina Island, California, USA) where
834 collections were attempted.

835

836 **Figure 2.** Diagrammatic representation of aquarium setup for Vargula tsujii . (A) Source water
837 flows into (B) a reservoir tank, which overflows to keep the reservoir full and water level
838 constant. (C) We use a siphon to carry water from a reservoir tank to main aquarium where
839 ostracods live. Water level of the main tank drains through sand (stippled), through (E) an
840 outflow that is raised to a level that would cause water to remain at the level of the dashed line,
841 even if a siphon is interrupted to cause water to stop flowing into the main tank. (F) Plastic bottle
842 and parts used to create small aquarium using the same logic as main aquarium. (G) Custom-
843 built acrylic aquarium with drain in bottom and raised outflow with adjustable rate.

844

845 **Figure 3.** Haplotype networks for (A) COI sequences, and (B) 16S sequences of *Vargula tsujii*
846 animals from three localities sampled. Abbreviations: CI, Catalina Island; SD, San Diego; SP,
847 San Pedro.

848

849 **Figure 4.** Embryogenesis within brooding females of *Vargula tsujii* post release into the
850 marsupium. (A) Day 0, (B) Day 1-4, (C) Day 5-7, (D) Day 8-9, (E) Day 10-13, (F) Day 14-17, (G)
851 Day 18-19, (H) Day 20-21, (I) Day 22-23, (J) Day 25-38.

852

853 **Figure 5.** Summary of the timing of embryogenesis stages in *Vargula tsujii*. This represents the
854 complete range of first appearance of each features across multiple broods, including: yolk
855 separation (range = 5-8 days, N = 7); eye spot formation (range = 10-18 days, N = 12); upper lip
856 formation (range = 15-19 days, N = 3); limb formation (range = 18-23 days, N = 11); hatching
857 (range = 25-38 days, N = 11).

858

859 **Figure 6**. Images of selected individuals within each inferred instar stage: (A) A-V, (B) A-IV, (C)
860 A-III, (D) A-II, (E) A-I male, (F) A-I female, (G) Adult male, (H) Adult female.

861

862 **Figure 7.** (A) KMeans clusters of *Vargula tsujii* developmental stages based on carapace height
863 and width. Instar stages were assigned to each cluster via comparison to *P. annecohenae* and
864 additional analysis of male and female size dimorphism. (B) Points representing laboratory
865 cultured animals overlayed on wild caught and unknown data. Different colors represent
866 different clusters in the KMeans analysis, and are labeled with their inferred instar/adult stages.
867 (C) Shows wild-caught animals dissected and identified as female in relation to the KMeans
868 clusters, and (D) shows wild-caught animals dissected and identified as male in relation to the
869 KMeans clusters.

870

871 **Figure 8.** Plot of length versus eye to keel distance (EKD) in animals assigned to the A-I
872 Instar/Adult Male cluster in the previous KMeans analysis (Figure 7A). These points were then
873 clustered via KMeans analysis into three clusters, which we assigned to A-I Males (red), A-I
874 Females (blue), and Adult Males (yellow).

875

876 **Figure 9.** Mitochondrial genome of *Vargula tsujii*. Note the duplicated control regions, CR1 and
877 CR2 (in gray). Figure produced with Circos [78].

878

879 **Supplementary Materials**

880 **Table S1.** List of collections locations or attempted collection locations for *Vargula tsujii*.
881 Collection locations for which a latitude and longitude could not be determined were not figured,
882 but are included here.

883

884 **Table S2.** List of specimens examined in this paper for which sequences were obtained,
885 including locality, museum collection numbers (where applicable), and GenBank accession
886 numbers for the two genes sequenced (COI and 16S).

887

888 **Table S3.** Raw measurements of *Vargula tsujii* individuals, including carapace height and
889 length, keel width and eye width.

890

891 **Table S4.** Unfiltered library sequencing statistics for *V. tsujii*.

892

893 **Figure S1.** Traversal of the cleaned SPAdes *V. tsujii* mitochondrial genome assembly graph
894 nodes plotted by Bandage (gray). The single circularizing path representing the collapsed
895 duplicate control regions are shown in blue. The black stroke shows the path traversed through
896 the assembly graph followed to produce the circularized mtDNA FASTA file with two control
897 region, matching the structure of the V. hilgendorfii mtDNA (Ogoh and Ohmiya 2004).

898

899 **Figure S2.** Results for our 16S DAPC model test to determine the number of clusters that is
900 favored via comparison of Bayesian Information Criterion (BIC) values.

901

902 **Figure S3.** Results for our COI DAPC model test to determine the number of clusters that is
903 favored via comparison of Bayesian Information Criterion (BIC) values.

904

905 **Figure S4.** Cluster membership based on our 16S DAPC analysis compared with the original
906 population designation for each specimen. Overall, the clusters are not representative of any
907 population-level structure.

908

909 **Figure S5.** Cluster membership based on our 16S DAPC analysis compared with the original
910 population designation for each specimen. Overall, the clusters are not representative of any
911 population-level structure.

912

913 **Figure S6.** Exploded diagram of custom aquarium for rearing *Vargula tsujii*. A photo of built
914 aquarium is in main text, Figure 2. **A**. Plumbing components include 1. PVC pipe 1.5 inch
915 diameter. 2. PVC socket ball valve to control the rate of outflow 3. PVC 1.5 inch elbows 4. PVC
916 elbow with one side threaded to screw into 5. threaded bulkhead to span bottom of aquarium for
917 drainage 6. float switch valve to control water level (not shown on Figure 2 of main text). **B**.
918 Acrylic panels of ¼ inch thickness welded together with solvent include 7. Two panels of
919 dimension 16.5 x 13.25 inches that form the long sides of the aquarium 8. Two panels of
920 dimension 8 x 10.75 inches that form the short sides of the aquarium. One of these panels has
921 a hole drilled for the water inflow and float switch 9. One panel of 16.5 x 7.5 inches to form the
922 bottom of the aquarium, including a hole drilled for the bulkhead 10. One panel of 16.5 x 7.5
923 inches to forms a false bottom for the aquarium similar to the bottom of an undergravel
924 aquarium filter. We drilled small holes throughout to allow water but not sand to flow through.
925 (Not shown on Figure 2). In practice, we welded legs on the false bottom to allow it to stand on
926 the true bottom of the aquarium above the height of the bulkhead drain.

927

928 **Figure S7**. Small aquarium ("condo") setup using an inverted 500 ml bottle. a. Seawater feed
929 through a hose into reservoir tank. b. Inverted bottle with hole in bottom and tube piercing

septum cap c. Siphon to bring water to condo (note in this staged example for photo, reservoir tank level is higher than condo, so water would flow out the top of the condo) d. Reservoir tank receives water from inflow and overflows e. Stand to hold condos f. Outflow tube using ¼ inch aquarium tubing, raised to set water level.